Electrical Engineering
https://doi.org/10.1007/s00202-024-02239-5

ORIGINAL PAPER

Coal power plant-enabled grid resilience through distributed energy resources and demand response integration

Vivek Saxena[1,2] · Narendra Kumar[1] · Uma Nangia[1]

Received: 13 September 2023 / Accepted: 2 January 2024

Abstract
In the growing world, the utilization of electrical energy is increasing rapidly. Excessive use of fossil fuels will drain them and also invite hazardous pollution. Integrating renewable energy resources as distributed generators (DGs) can fulfill the rapidly increasing electrical energy demand and promote green energy generation to a large extent. The intermittent nature of renewable energy and higher penetration of DG may adversely affect the operation of the distribution network (DN). As a result, power disparity, reverse power flow to the grid, and voltage instability may exist. One key solution is to optimally integrate the renewable energy-based DG and battery energy storage system (BESS) in the coordination of demand response (DR). This paper proposes a multilevel particle swarm optimization technique to synchronize the distributed energy resources (DER) and DR in the DN. The proposed approach is implemented on the IEEE 33 bus system energized by coal power plant (CPP). The first level of optimization finds the sizes and locations of DER (DG and BESS), and the next level determines the optimal power dispatch in the coordination of DR. The outcomes of this framework exhibit effectiveness in the optimal utilization of renewable energy resources and the enhancement of power quality parameters in DN so that CO_2 emissions are reduced by 32.71% from CPP.

Keywords CO_2 · Coal power plant · Distributed generation · Demand response · Renewable energy · Battery energy storage system · Multilevel optimization

List of symbols

t.p.	Time period
P_i^T, P_J^T	Active power magnitude ith and jth node for the t.p. of T
r_{ij}	Branch resistance between ith and jth node
$P^T_{\mathrm{BESS}\left(\frac{C_i}{D_i}\right)}$	Power of BESS (charging and discharging) at ith node for t.p. of T
I^T_{Grid}	Output current the substation transformer at any time T
$P^{\mathrm{Max.}}_{\mathrm{BESS}}$	Maximum limit of power dispatch
Ψ	Conversion factors from daily to yearly
η_c	Charging efficiency of BESS
P_c^T	Converter loss for t.p. of T
I_{ij}^T	Level of current between i and j bus in hour T
η_d	Discharging BESS efficiency
$P_{\mathrm{PV}}^{\max}$	Maximum size of DGs
$E_{\mathrm{BESS},i}$	BESS energy at ith node
V_{Max}, V_{Min}	Limits of node voltages
η	Efficiency of the storage system
$P^{\mathrm{Min.}}_{\mathrm{BESS}}$	Minimum limit of power dispatch
V_i^T	Magnitude of the voltage at the ith node during the t.p. of T
V^T_{Grid}	Magnitude of grid voltage at any time T
$E^{\mathrm{Max}}_{\mathrm{BESS}}$	Maximum limit of energy
C	Contract load
$I_{ij}^{\max}$	Thermal limit (maximum) of line between bus i and j (A)
K_i^T	Allocated load factor for bus i at t.p. of T
$P_{\mathrm{el},i}^{\min}$, $P_{\mathrm{el},i}^{\max}$	Limits of responsive load (maximum and minimum)

✉ Vivek Saxena
vvksaxena1234@gmail.com

[1] Department of Electrical Engineering, Delhi Technological University, New Delhi, India

[2] Department of Electrical and Electronics Engineering, A.B.E.S. Engineering College, Ghaziabad, India

Published online: 29 January 2024

V_i^T, V_j^T	Node voltage of *i*th and *j*th node for the t.p. of T
$P_{\text{in},i}^T$	Instantaneous load (nonresponsive and responsive)
Q_{Di}^T	Reactive power demand at node *i*th at any time T
P_{Loss}^T	Power delivery loss for the t.p. of T
Q_i^T, Q_j^T	Reactive power magnitude *i*th and *j*th node for the t.p. of T
R_{PV}^r	Rated PV module radiations
$P_{\text{el},i}^T$	Responsive load at any time T
P_{Di}^T	Real power demand at node *i*th at any time T
E_i^{Total}	Total demand of energy of the day
$\text{SOC}^{\text{Min.}}$, $\text{SOC}^{\text{Max.}}$	SOC limits
P_{Gi}^T	Real power injection at node *i*th
R_{PV}^T	Solar radiation at time T
χ	Penetration of DR
SOC_i^T	SOC of BESS at bus i in hour T
$P_{\text{PV},i}$	Active power injection at node *i*th at any time T
V_D^T	Voltage deviation penalty
I_{Spc}	Specified reverse current limit
P_R^T	Reverse power flow at any time T
Δt	Change in time
I_{PV}	Solar module current (A)
δ_i^T, δ_j^T	Voltage angle of *i*th and *j*th node for the t.p. of T
Q_{Gi}^T	Reactive power injection at node *i*th for any time T
$L_{d,i}^T$	Hourly demand for the t.p. of T
$P_{D,i}^0$	Initial real power demand at *i*th node
$Q_{D,i}^0$	Initial reactive power demand at *i*th node
N	Number of buses

1 Introduction

In the modern age, the integration of renewable energy resources demands the implementation of a smart grid, utilizing real-time information and advanced communication technologies to achieve its objectives. Smart grids enable bidirectional communication between energy consumers and producers [1]. Several studies have investigated responsive load management based on dynamic pricing, all arriving at the same conclusion: shifting energy consumption from peak to off-peak hours in coordination with renewable energy resources maximizes benefits for prosumers [2–4]. Rapid advancements in small-scale generation technologies have compelled distribution system operators (DSOs) to increase the proportion of distributed generators (DGs) in distribution networks (DN). To optimize DN performance, it is essential to determine the ideal size and location of DGs. Previous research has demonstrated that suboptimal resource allocation can have counterproductive effects [5–7].

By incorporating DGs optimally, various objectives have been achieved, such as enhancing power quality, improving voltage profile, reducing atmospheric pollutants, and enhancing system stability and reliability, among others. However, traditional distribution systems face challenges in handling a large number of renewable energy sources due to their uncontrollable and unpredictable nature, which also varies over time [8].

To address this, one potential solution is the adoption of battery energy storage systems (BESS) to increase the penetration of power from non-dispatchable DGs in the DN [9–12]. Many studies have focused on modeling and optimizing the energy management of BESS to support DG integration.

While considerable efforts have been made to optimize BESS capacity, the location aspect is often overlooked in the objective function [9, 10]. To fully optimize DN performance, it is highly recommended to simultaneously consider both the location and size of BESS, which currently lacks adequate attention in the academic literature. By identifying the optimal size and position of BESS, the benefits of DSOs can be significantly enhanced [11].

The optimization of BESS involves various objectives, including minimizing power losses, depreciation of cost functions, and maximizing energy arbitrage profits, as discussed in [12]. The study evaluates the implications of optimizing the capacity and location of BESS for hybrid power plants based on wind energy and hydro energy in coordination with BESS, as stated in [13].

In their research [14], the authors explored how network reconfiguration influences the sizing and placement of BESS. However, implementing BESS can be costly for the DSO, leading to increased investment and operational expenses. The lifespan of BESS is influenced by factors such as the depth of discharge (DOD) and charging and discharging cycles, as mentioned in [15]. Studies indicate that a well-positioned and sizable BESS can support high penetration of DGs. Yet, expanding the BESS size can create additional cost burdens for the DSO, prompting researchers to explore alternative methods for DR to alleviate this pressure on BESS. DR has shown promise in various aspects of the smart grid, including communication and consumer coordination through price-based demand response, leading to reduced energy consumption costs and peak occurrence [16]. DR implementation in the DN in Finland resulted in technological benefits like reduced power losses and improved voltage profiles [17]. Researchers demonstrated a DR-coordinated

approach in allocating DGs to mitigate the intermittent nature of renewable energy sources [18–21].

The authors have effectively showcased the efficiency and advantages of integrating renewable energy planning into the coordinated management of electric vehicles [22, 23]. This integration not only contributes to the optimization of the DN but also emphasizes the intersection of technological advancements and economic benefits. To realize these synergies within the DN, the study employs sophisticated bilevel or multilevel optimization approaches [24–26]. These approaches, characterized by their hierarchical structure, enable a comprehensive exploration of technological and economic optimizations in hybrid energy systems [27–30].

Furthermore, the study recognizes the pivotal role of DER in enhancing the power grid's overall performance. The integration of DER into the power grid has been documented to significantly improve various power quality parameters [31–33]. This underscores the broader impact of incorporating DER technologies, such as renewable energy sources, in bolstering the reliability and quality of the electrical power supply.

DR is implemented to address demand and supply imbalances and mitigate the constraints faced by DG owners. In a previous study by the authors [34], they explored the joint deployment of DR and DG loads in the DN. The authors demonstrated a coordinated approach to optimize the benefits for various stakeholders in the utility sector [35, 36]. Based on this research, it was found that DR proves effective in scenarios with regulated loads, dynamic pricing, and renewable resources. After an extensive analysis of relevant published research, the authors concluded that integrating DGs and BESS into distribution networks significantly improve network efficiency. DR facilitates a high penetration of DGs and provides substantial advantages to smart grid participants, including customers, DSOs, generating firms, and aggregators. Although previous research has explored the optimal allocation of DGs when coordinating with DR, the incorporation of BESS in this context remains understudied. Hence, the objective of this research is to examine the role and benefits of DR in effectively integrating DGs and BESS in the DN. A key factor influencing the effectiveness of DR is consumer participation levels. Therefore, the study aims to determine how DR rates impact the appropriate sizing and placement of solar photo voltaic (SPV) and BESS systems. To achieve this, a multilevel optimization framework is utilized to seamlessly integrate PVs and BESS with DR planning in the DN.

According to the report released by the Central Electricity Authority (CEA) in 2022, the carbon dioxide (CO_2) emission from coal power plants (CPP) in the Indian power sector is 0.975 tCO_2/MWh [37]. To reduce these emissions, strategically placing renewable DG in the DN is essential. In this paper, SPV is considered as the renewable DG, known for its pollution-free electricity production. However, it is crucial to note that CO_2 emissions occur during the construction of SPV plant components, as they rely on electricity from thermal power plants. For SPV modules, the estimated lifetime CO_2 emission is 0.053 kg per 1 kWh of electrical energy [38].

Figure 1 shows the capacity additions from financial year (FY) 2000–2001 to FY 2021–2022. Notably, coal-based capacity witnessed substantial growth from FY 2000–2001 to FY 2015–2016, but there was a significant decline in capacity additions from FY 2016–2017 to FY 2021–2022. Hydro-based capacity additions also experienced a notable decrease starting from FY 2017–2018. No recorded additions were observed in other generation capacities during this period.

Figure 2 illustrates the trend of the weighted average emission factor from FY 2017–2018 to FY 2021–2022. During FY 2021–2022, there was a slight increase in the weighted average emission factor, primarily due to a rise in total electricity generation, with approximately a 2% increase in coal-based generation. However, there was a minor reduction in gas and hydro-based generation. Additionally, the proportion of imported coal decreased from 9 to 4% compared to the previous fiscal year.

This research paper encompasses several objectives, including minimizing feeder energy losses and BESS energy conversions, reducing voltage deviations, and minimizing reverse power flow while maximizing the use of BESS and DR in the presence of high SPV penetration. So that the CO_2 emission can be reduced effectively. To assess the effectiveness of proposed framework, numerous test scenarios have been examined to a typical 33-bus test data set and the power grid is supplied by CPP.

2 Problem conceptualization

Effectively increasing the adoption of renewable energy sources and optimizing energy efficiency can lead to substantial reductions in CO_2 emissions. By reducing the electricity demand from conventional CPP, significant CO_2 emissions can also be curtailed.

In this study, the following objectives have been examined for the optimal allocation of PV and BESS in the effective synchronization of DR panning in DN.

2.1 Minimization of power losses

Power losses during power transmission in DN are considerable. Implementing technological advancements like integrating DGs, optimizing BESS functionality, and coordinating DR offer substantial potential for reducing these losses. Minimizing power loss is a crucial goal function, as it

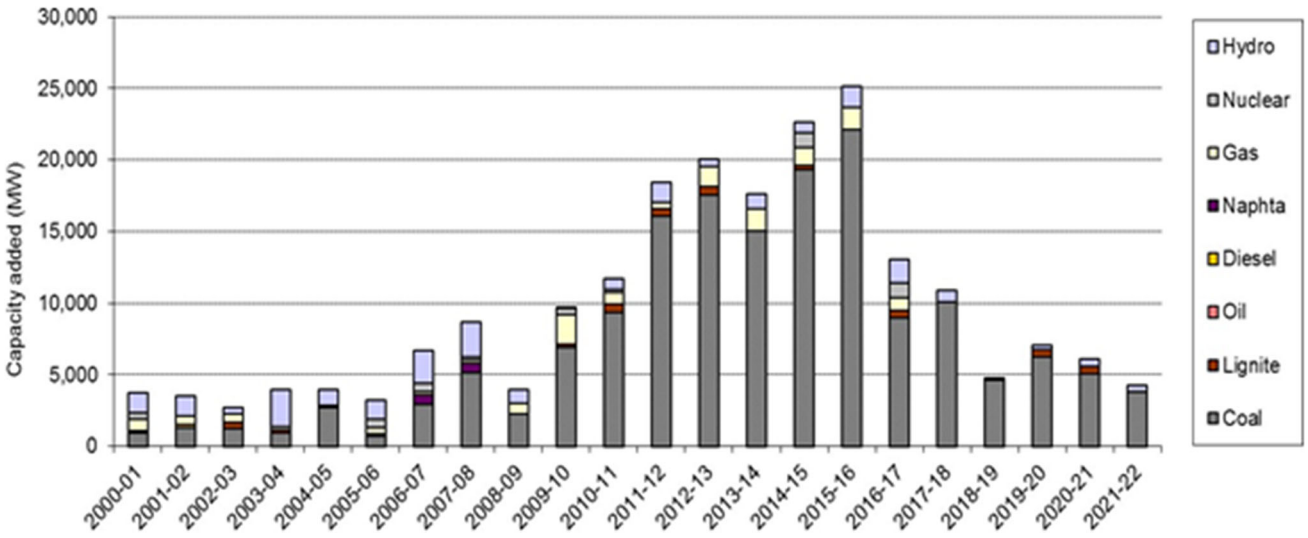

Fig. 1 Breakdown of new added capacity covered by the database over the period 2000–2001 to 2021–2022 [37]

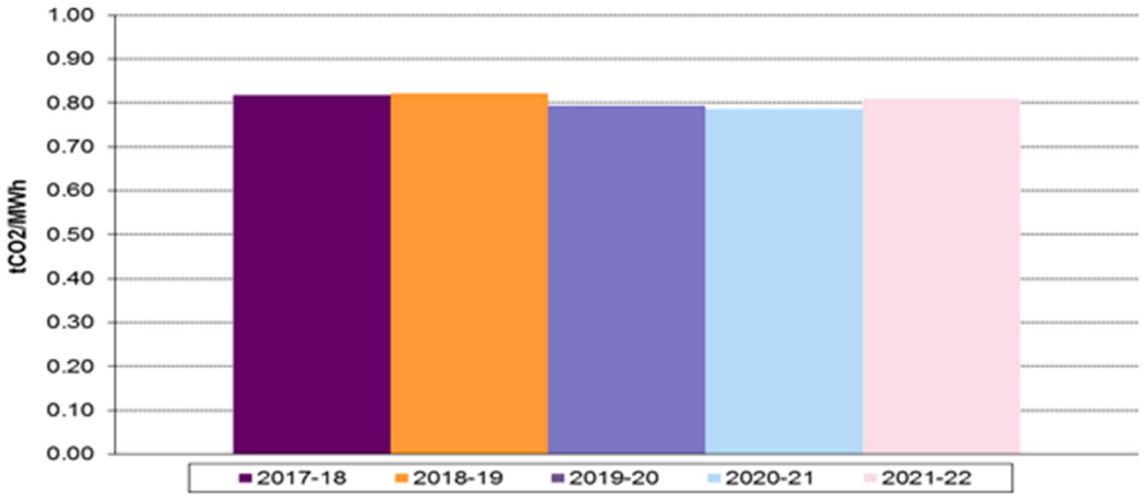

Fig. 2 Development of the weighted average emission factor for the Indian Grid over the period 2017–2018 to 2021–2022 [37]

directly affects the annual income of utilities and has implications for all stakeholders [39].

$$f_1 = \sum_{T=1}^{24} P_{\text{Loss}}^T \tag{1}$$

$$P_{\text{Loss}}^T = \sum_{i=1}^{N}\sum_{j=1}^{N} \alpha_{ij}^T \left(P_i^T P_J^T + Q_i^T Q_J^T\right) + \beta_{ij}^T \left(Q_i^T P_j^T - P_i^T Q_j^T\right) \forall T \tag{2}$$

where $\alpha_{ij}^T = r_{ij}\cos\left(\delta_i^T - \delta_j^T\right)/V_i^T V_j^T$ and $\beta_{ij}^T = r_{ij}\sin\left(\delta_i^T - \delta_j^T\right)/V_i^T V_J^T$.

2.2 Minimization of reverse power flow

Anticipated rise in renewables to meet green energy targets and reduce emissions. Increasing penetration may cause reverse power flow during low demand, posing operational complexity and protection challenges for DSOs. DG integration aims to address this reverse flow possibility. The goal: achieving bidirectional power flow.

$$f_2 = \sum_{T=1}^{24} P_R^T \tag{3}$$

$$P_R^T = \begin{cases} 0, & \text{if } I_{\text{Grid}}^T \geq I_{\text{Spc}} \\ \text{Re}\left(V_{\text{Grid}}^T I_{\text{Grid}}^{T*}\right) & \text{if } I_{\text{Grid}}^T < I_{\text{Spc.}}. \end{cases} \tag{4}$$

2.3 Minimization of BESS conversion losses

Recent research has extensively focused on converters and battery storage systems. To ensure efficient integration of BESS, it is crucial to minimize converter losses. As a result, one of the objectives is to consider the conversion losses during the charging and discharging periods of BESS. The formula for BESS loss is as follows:

$$f_3 = \left(\sum_{T=1}^{24} P_c^T \right) \tag{5}$$

$$P_c^T = (1-\eta) P^T_{\mathrm{BESS}\left(\frac{C_i}{D_i}\right)} \tag{6}$$

2.4 Node voltage deviation

To maintain power supply reliability, the DN must operate within an acceptable voltage range. Typically, a penalty function is used to account for voltage violations. This penalty function can also be considered as one of the objectives.

The purpose of exceeding the voltage limit can be stated as follows [40]:

$$f_4 = \left(1 + \sum_{T=1}^{24} V_D^T \right) \tag{7}$$

$$V_D^T = \begin{cases} \left| V_{\mathrm{Min}} - V_i^T \right| & \text{if } V_i^T < V_{\mathrm{Min.}} \\ 0 & \text{if } V_{\mathrm{Min.}} \le V_i^T \le V_{\mathrm{Max.}} \\ \ell & \text{if } V_i^T > V_{\mathrm{Max.}} \end{cases} \tag{8}$$

$\boldsymbol{l}$ denotes an arbitrarily large positive integer. A high value represents an unfavorable solution, particularly when it comes to voltage rise beyond the maximum working limit, which poses a significant problem [41]. The issue of voltage rise intensifies during low demand, potentially leading to equipment failure due to insulation collapse and impact on protection measures. The increasing voltage poses a major obstacle to deeper DG penetration in the DN. To address this, a hard constraint is imposed to prevent violations of the higher voltage limit. Conversely, the minimum voltage is treated with more flexibility, allowing slight deviations as long as an appropriate penalty factor is applied.

2.5 Fitness function

To achieve the required objectives, it is required to make a fitness function having the weightage factor of different objective functions. For level 1 of optimization, the fitness function ($F_{\ell 1}$) is given as:

$$\min(F_{\ell 1}) = \Psi \times L \times f_4 \tag{9}$$

where $L = f_1 + f_2 + f_3$.

The level 2 of the optimization objectives involves taking into consideration the DR planning and scheduling methods of DGs and BESS. In this stage, the BESS conversion losses are irrelevant and have no impact. Because of this, the following objective function will be taken into consideration for level 2 of the optimization problem:

$$\min(F_{\ell 2}) = \kappa \times f_4 \tag{10}$$

where $\kappa = f_1 + f_2$.

In this context, the fitness function for level 2 is denoted by $F_{\ell 2}$.

It is vital to have a dispatch strategy, which is determined upon by the DR aggregator. This helps to minimize the aforementioned goal function.

2.6 Demand response aggregator

The developed DR system considers the benefits enjoyed by various stakeholders, including DSOs and consumers. The DR aggregator influences customers' demand scheduling based on their participation in DR, subject to technological limitations. This study primarily focuses on the technological challenges caused by the widespread use of SPVs. DR implementation uses dynamic tariff information to schedule loads and achieve maximum reduction in set technical targets, without considering financial objectives. Participants in mandatory DR programs may face financial penalties for not following the aggregator's instructions. The scheduling of demand aims to balance total consumption and available resources throughout the day, restructuring demand instead of simply reducing overall consumption.

The DR aggregator schedules load by collecting information on responsive and nonresponsive load demand, making it an essential part of the program.

Responsive load demand refers to the electricity demand that can be adjusted or shifted in response to instructions from the DSO. On the other hand, nonresponsive load demand denotes the electricity demand that cannot be altered or shifted from its usual operating hours. Essentially, responsive loads provide flexibility in their consumption patterns, allowing for adjustments to optimize the overall performance and efficiency of the electrical grid, particularly in scenarios where the DSO seeks to balance supply and demand or manage grid constraints. In contrast, nonresponsive loads maintain a fixed demand profile, typically adhering to their established operating schedules without the capacity for immediate adjustment based on external instructions. Equation (13) represents the complete demand at any time T, which

is the sum of all types of loads (responsive and nonresponsive). To meet responsive demand without affecting overall daily demand, scheduling restrictions are defined in Eq. (14), with Eq. (15) representing the minimum and maximum values of responsive demand. The peak value of responsive demand depends on the penetration level of DR, as shown in Eq. (16). Various DR restrictions are considered, as discussed in [42].

$$P_i^T = \left(P_{Gi}^T - P_{Di}^T\right)\forall T,\ i \tag{11}$$

$$Q_i^T = \left(Q_{Gi}^T - Q_{Di}^T\right)\forall T,\ \mathrm{I} \tag{12}$$

$$P_{Di}^T = \left(P_{\mathrm{in},i}^T + P_{\mathrm{el},i}^T\right)\forall T,\ i \tag{13}$$

$$\sum_{i=1}^{N}\sum_{T=1}^{24}\left(P_{\mathrm{in},i}^T + P_{\mathrm{el},i}^T\right) \times \Delta t = E_i^{\mathrm{Total}} \tag{14}$$

$$P_{\mathrm{el},i}^{\min} \le P_{\mathrm{el},i}^T \le \min\left(\left(C - P_{\mathrm{in},i}^T\right),\ P_{\mathrm{el},i}^{\max}\right)\forall T \tag{15}$$

$$P_{\mathrm{el},i}^{\max} = \chi \sum_{T=1}^{24} L_{d,i}^T \tag{16}$$

The optimal solution to the optimization issue is a vector of responsive load schedules with a length of T and is represented as:

$$P_{\mathrm{el}} = \left[P_{\mathrm{el}}^1,\ P_{\mathrm{el}}^2,\ P_{\mathrm{el}}^3,\ P_{\mathrm{el}}^4 \cdots P_{\mathrm{el}}^T\right]\forall T.$$

2.7 Objective constraints

The objective functions are constrained in a variety of ways by both technical and operational considerations. These restrictions can be represented numerically as follows:

2.7.1 SPV generation limit constraint

The constraint for PV generation limit is given as:

$$0 \le P_{\mathrm{PV},i} \le P_{PV}^{\max}\forall i \tag{17}$$

2.7.2 BESS constraints

The constraints of BESS are given as:

$$0 \le E_{\mathrm{BESS},i} \le E_{\mathrm{BESS}}^{\mathrm{Max}}\forall i \tag{18}$$

$$P_{\mathrm{BESS}}^{\mathrm{Min.}} \le P_{\mathrm{BESS}(C_i/D_i)}^T \le P_{\mathrm{BESS}}^{\mathrm{Max.}}\forall T,\ i \tag{19}$$

$$\mathrm{SOC}^{\mathrm{Min.}} \le \mathrm{SOC}_i^T \le \mathrm{SOC}^{\mathrm{Max.}}\ \forall T,\ \mathrm{I} \tag{20}$$

$$\mathrm{SOC}_i^T = \begin{cases} \mathrm{SOC}_i^{T-1} + P_{\mathrm{BESS}(\mathrm{C}_i/\mathrm{D}_i)}^T \eta_c \Delta t / E_{\mathrm{BESS}}^R & \text{if } P_{\mathrm{BESS}(\mathrm{C}_i/\mathrm{D}_i)}^T > 0 \\ \mathrm{SOC}_i^{T-1} + P_{\mathrm{BESS}(\mathrm{C}_i/\mathrm{D}_i)}^T \Delta t / \eta_d E_{\mathrm{BESS}}^R & \text{else} \end{cases} \tag{21}$$

$$\sum_{T=1}^{24} \eta_c P_{\mathrm{BESS}(C_i/D_i)}^T + P_{\mathrm{BESS}(C_i/D_i)}^T / \eta_d = 0 \tag{22}$$

Equation (18) represents the limitations of energy while Eq. (19) represents the limitations of power dispatch. The limits of SOC are given in Eq. (20), and SOC status is presented in Eq. (21). SOC balancing constraints are demonstrated in Eq. (22). All the above equations are at specific node and time.

2.7.3 Feeder constraint

The constraint for the thermal limits is given as:

$$I_{ij}^T \le I_{ij}^{\max}\forall T,\ i,\ j \tag{23}$$

2.7.4 Power balance constraints

$$P_i^T = V_i^T \sum_{j=1}^{n} V_j^T Y_{ij} \cos\left(\theta_{ij} + \delta_j^T - \delta_i^T\right)\forall T,\ i \tag{24}$$

$$Q_i^T = -V_i^T \sum_{j=1}^{N} V_j^T Y_{ij} \sin\left(\theta_{ij} + \delta_j^T - \delta_i^T\right)\forall T,\ i \tag{25}$$

The actual and reactive power balance restrictions are shown by Eqs. (24) and (25), respectively.

2.8 Demand modeling

The demand modeling of the system is given in the following equations:

$$P_{D,i}^T = \kappa_i^T P_{D,i}^0 \forall T,\ i \tag{26}$$

$$Q_{D,i}^T = \kappa_i^T Q_{D,i}^0 \forall T,\ i \tag{27}$$

2.9 SPV generation modeling

Solar power generation is dependent on a number of other factors as well, such as the type of panel and its area, the angle at which it is tilted, and the amount of solar radiation that is received. For the purposes of this study, during a specific

period of time, it is assumed that all other parameters remain unchanged. The transformation of the current in relation to the rated voltage may be found as follows:

$$I_{\mathrm{pv}}^{T} = \begin{cases} I_{\mathrm{PV}} & \text{if } R_{\mathrm{PV}}^{T} \geq R_{\mathrm{PV}}^{r} \\ I_{\mathrm{PV}} \times R_{\mathrm{PV}}^{T}/R_{\mathrm{PV}}^{r} & \text{if } R_{\mathrm{PV}}^{T} < R_{\mathrm{PV}}^{r} \end{cases} \tag{28}$$

3 Optimization technique

As discussed in previous case, the presented optimization objectives required such a optimization technique that can solve the complex nonlinear problem. The adoption of a multilevel optimization context is required by the presence of BESS since it takes into consideration both the limits associated with SOC levels and their accessibility. The optimal allocations of PVs and the BESS are determined at the first level of optimization. At the second level of optimization, the hourly power scheduling of BESS in the synchronization of DR programs is determined. This is done to make sure that the operational gains from DSO are used to their fullest extent.

Any evolutionary method can be utilized to address the difficult multilevel optimization issue that has to be solved. According to a review of the relevant published material, it has been determined that PSO is the method that is utilized most frequently for tackling the DG planning optimization problem [43]. As a result, the optimization goal presented in this work has been met at both levels by using PSO.

The PSO is an optimization approach that has the capability to search for a global or near-global solution to difficult optimization issues involving power systems, and it is a particle-based meta-heuristic technique. Here are the things that need to be done to improve the multilevel optimization that is being thought about:

I. Set the initial values for the parameters and variables that are used in level 1 optimization. It includes locations, sizes of PVs and BESS, and parameters of the proposed optimization technique.
II. Upgrade the sizes and locations of PV that have been determined heuristically.
III. Apply the calculated load factor κ_i^T to the P_{Di}^T and Q_{Di}^T for a period of 24 h.
IV. The level 2 gets the most up-to-date location, size of BESS P_{Gi}^T, P_{Di}^T, and Q_{Di}^T so that BESS and DR can be managed as well as possible.
V. For the level 2, the arrangement of responsive load and BESS power dispatch over a period of twenty-four hours is seen as the variables.
VI. At the level 2, the scheduling of BESS and DR is started subsequently getting the outcomes from first level subjected to various constraints of the system.
VII. Execute the load flow to find out how much power is lost and how much voltage is at each node.
VIII. Perform another round of updates to P_{Gi}^T (BESS discharging) and P_{Di}^T (BESS charging and also depends on the planning of responsive loads) in accordance with the BESS and DR schedules that were optimized in level 2.
IX. The level 1 controller receives upgraded variables like P_{Gi}^T, P_{Di}^T, SOC, and BESS power in order to optimize the objective of Eq. (9).
X. Perform the load flow to find out the energy losses in addition the level of voltages at different nodes, it is necessary to evaluate the performance of level-1 optimization function.
XI. Preserve the level 1 population with the highest fitness and its matching best population.

The flow-chart that is given in Fig. 3 illustrates both the upper and lower levels' structures in great detail.

The scheduling of BESS will depend upon the optimized value of dispatch power and the present value of SOC. The value of DOD is assumed to be 20% of the peak value of DOD and, primarily, the value of SOC is equal to the value of DOD. The optimal power dispatch and SOC will determine how the BESS charges and drains.

4 Results and discussion

The proposed multilevel optimization technique is implemented on the IEEE 33 bus system as shown in Fig. 4 [44]. In this research, the effects of DR technologies are shown and analyzed in order to solve the optimal power dispatch problem in a number of different scenarios and with a number of different constraints. The optimization objectives are solved with the help of proposed optimization techniques by using MATLAB software on i3 core processor having 12 GB RAM. PV is considered as DG during the optimal planning of power dispatch with the coordination of BESS and different DR rates. The details about the simulation settings for the multilevel optimization are given in Table 1. Additionally, the values of base voltage, nominal active demand, nominal reactive demand, power loss, $V_{\min}$, $V_{\max}$, $P_{\mathrm{BESS}}^{\mathrm{Min}}$, $P_{\mathrm{BESS}}^{\mathrm{Max}}$, $\mathrm{SOC}^{\mathrm{Min}}$, $\mathrm{SOC}^{\mathrm{Max.}}$, $\mathrm{DG}^{\mathrm{Max.}}$ and $E_{\mathrm{BESS}}^{\mathrm{Max}}$ are 12.66 kV, 3715 kW, 2300 kVAr, 202.7 kW, 0.95 pu., 1.05 pu, − 1 MW, 1 MW, 0,1, 2 MW and 5 MWh, respectively.

Table 2 demonstrates how the DR rates impact the overall performance of the DN. The participation of different customers in various DR programs is reflected in the various DR

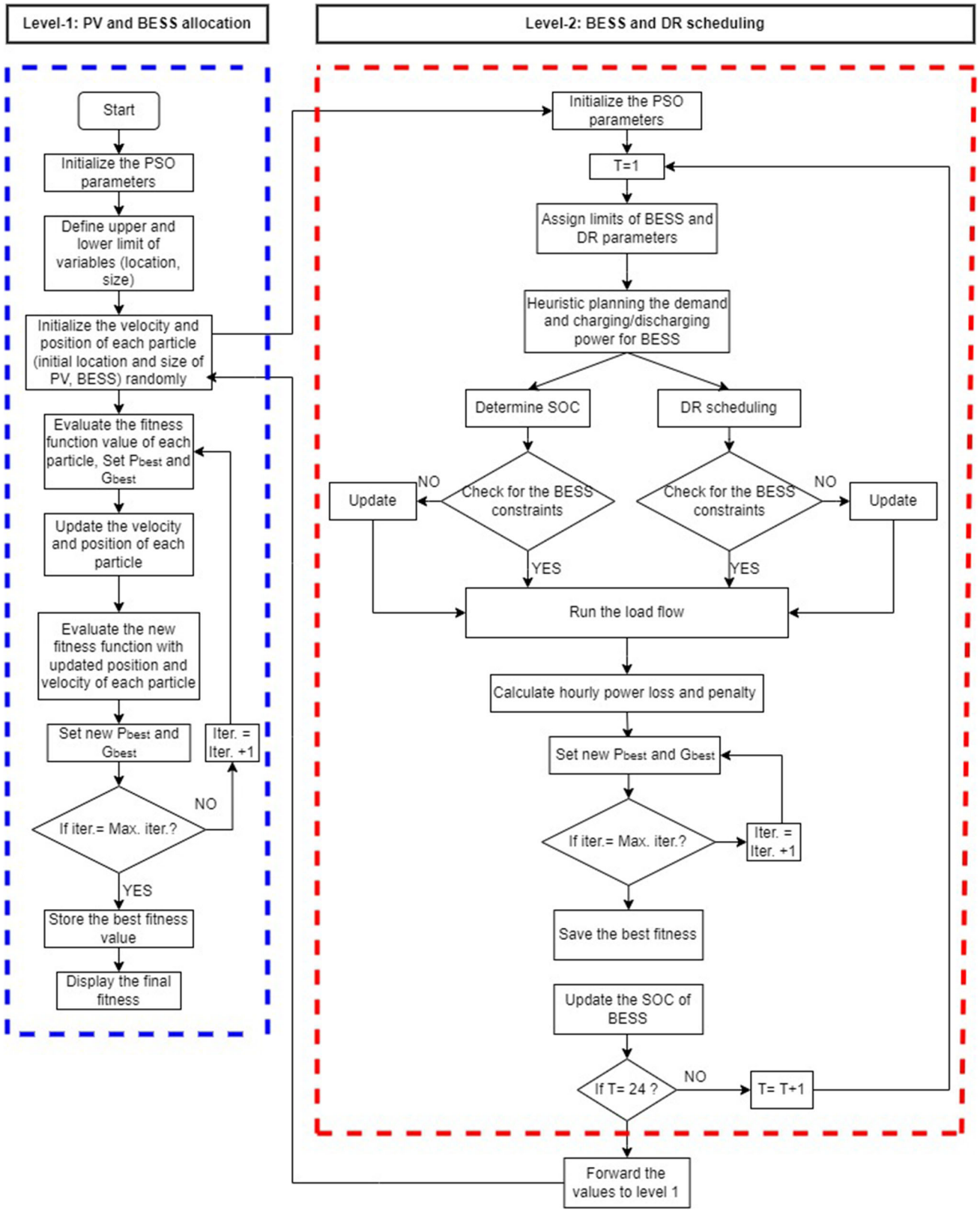

Fig. 3 Flow-chart for multilevel optimization approach

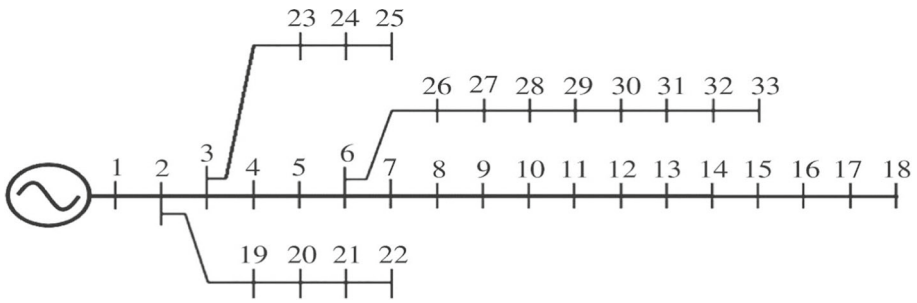

Fig. 4 IEEE 33 bus system

Table 1 Simulation parameters of multilevel optimization technique

Parameters	Level-1	Level-2
Swarm size	20	50
Inertia weight	1	1
Inertia weight damping ratio	0.99	0.99
Personal learning coefficient	1.5	1.5
Global learning coefficient	2	2
Maximum number of iterations	50	50

rates. In this case study, we are assuming that type DR programs are required. Participants in mandated DR programs are required to pay the fine/penalty if they did not coordinate their usage in accordance with the DR aggregator's instructions.

As a result, it is essential for the DR aggregator to monitor, control, and advise the consumers on scheduling the demand in accordance with the implemented DR rate. The outcomes of the optimal planning of power dispatch in the coordination of DG, DR, and BESS are given in Table 3. Once the recommended technique is put into place, significant reductions in yearly energy loss, reverse power flow, and voltage variations are seen. As an illustration of the effectiveness of the suggested technique, we present several case studies and their respective results. The proposed approach has a noteworthy impact on the CO_2 emissions of the CPP, as clearly outlined in Table 4.

4.1 Case 1

The purpose of discussing this scenario is to showcase the effectiveness of the proposed approach. For this analysis, neither PV nor BESS is considered in the 33-bus radial DS. In this specific case, the DSO relies entirely on power from the grid. The daily consumption pattern, obtained from reference [45], is incorporated into the proposed objective functions for convenience and speed. Based on Table 2 and 3, the base scenario shows differences of 5397.73 kW between maximum and minimum demand, a minimum mean voltage of 0.978178 p.u., and yearly energy losses of 1426 MWh. The peak demand occurs around 20:00 in the evening, while the valley point is approximately at 5:00 in the morning. The total CO_2 emission per day is 75,446.33 kg.

Table 2 Effect of the coordination of DR with optimally integrated renewable DG and BESS on demand

Case no	Category	Maximum demand (kW)	Maximum demand mitigation %	Difference between maximum-to-minimum demand (kW)	% of maximum loss mitigation at 8:00 PM
1	Base Case	6519	0	5397.73	0
2	DG	6519	0	6016.39	0
3	DR@10%	5548	16.1	4166.14	36.09
	DR@20%	5321	18.42	3730.6	42.77
4	DG + DR@10%	5370	17.33	4322.87	33.69
	DG + DR@20%	4790	26.78	3540.31	45.69
5	DG + BESS	4355	33.23	4100.89	37.09
6	DG + BESS + DR@10%	3810	41.54	3299.7	49.38
	DG + BESS + DR@20%	3290	49.54	2498.53	61.67

Table 3 Outcomes of the coordination of DR with optimally integrated renewable DG and BESS

Case no	Category	Optimal allocation of DG (Bus No., kW)	Optimal allocation of BESS (Bus No., kWh)	Annual losses (MWh)	Reduced losses/year (%)	DG penetration (%)	Average voltage level (p.u.)
1	Base Case			1426			0.9781
2	DG	17(1344)-32(1690)-25(1092)		1098	23	68.76	0.9963
3	DR@10%			1302	8.69		0.9784
	DR@20%			1290	9.53		0.9785
4	DG + DR@10%	7(1086)-15(1902)-32(914)		996	30.15	65.03	0.9964
	DG + DR@20%	18(408)-29(1816)-11(1602)		934	34.5	63.76	0.9967
5	DG + BESS	18(1901)-30(1657)-7(1840)	13(2697)-33(4593)-16(3773)	810	43.19	89.96	1.0121
6	DG + BESS + DR@10%	16(1532)-32(1736)-26(1855)	16(4529)-33(4386)-18(982)	786	44.88	85.38	1.0123
	DG + BESS + DR@20%	17(998)-11(2024)-30(1747)	16(4591)-33(4388)-18(985)	724	49.22	79.48	1.0127

Table 4 Impact of proposed framework on CO_2 emission of CPP

Case	Energy demand from CPP/Day (kWh)	Energy supplied from DG/Day (kWh)	CO_2 emission from SPV (Kg)	Energy losses/day (kWh)	Energy supplied from CPP/Day (kWh)	CO_2 emission/Day (Kg) by CPP	Total CO_2 emission/Day (Kg)	% reduction in CO_2 emission/Day
Base Case	73,474			3906.85	77,380.85	75,446.33	75,446.33	
DG	52,681	20,793	1102.029	3008.22	55,689.22	54,296.99	55,399.02	26.51%
DR@10%	73,472			3567.12	77,039.12	75,113.15	75,113.15	0.30%
DR@20%	73,411			3534.25	76,945.25	75,021.62	75,021.62	0.49%
DG + DR@10%	50,684	22,790	1207.87	2728.77	53,412.77	52,077.45	53,285.32	29.31%
DG + DR@20%	54,498	18,976	1005.728	2558.90	57,056.90	55,630.48	56,636.21	24.87%
DG + BESS	48,640	24,834	1316.202	2265.00	50,905.00	49,632.38	50,948.58	32.47%
DG + BESS + DR@10%	48,640	24,834	1316.202	2161.60	50,801.60	49,531.56	50,847.76	32.60%
DG + BESS + DR@20%	48,640	24,834	1316.202	2079.45	50,719.45	49,451.46	50,767.67	32.71%

4.2 Case 2

In this case, the initial optimization level calculates the penetration level and locations of DGs while keeping the remaining information unchanged. According to Table 2 and 3, specific values for this scenario indicate the difference between maximum and minimum demand as 6016.39 kW, the minimum mean voltage as 0.99634 p.u., and the yearly energy losses as 1115 MWh. The peak demand remains constant, depicted in Fig. 2, owing to the difference in solar generation availability compared to peak demand occurrence. Another valley point observed from 10:00 to 15:00 is attributed to the increased penetration of DG, reducing grid demand.

The optimized integration of DGs significantly improves power quality parameters. Specifically, in this instance, yearly energy losses reduced by approximately 21.8%, and the minimum mean voltage increased from 0.978178 to 0.99634 p.u. Table 3 presents the optimal dimensions and placement of PV installations within DS. The impact of DGs on demand pattern, voltage pattern, and active power losses is illustrated in Figs. 5, 6, and 7, respectively. The CO_2 emission is reduced by 26.51% in comparison with base case scenario.

4.3 Case 3

In this specific scenario, the study focuses solely on evaluating the effectiveness of the DR approach without coordinating with DGs or BESS. Two different levels of demand elasticity, namely 10 and 20%, are considered as the DR rates. DR identifies the elastic load that can be adjusted to suit demand and pricing conditions, while the inelastic load remains constant. Introducing various elastic loads in DR significantly improve performance compared to the basic scenario. Peak demand is reduced by 14.72 and 18.32% for the 10 and 20% DR rates, respectively, and annual energy losses decrease between 5.96 and 8.2%. This confirms that DR leads to reduced energy losses and improved peak-to-valley difference, even without DG integration.

Figures 8 and 9 demonstrate the impact of a 10% DR rate on demand pattern, voltage pattern, and active power losses, respectively. Similarly, Figs. 10 and 11 show the impact of a 20% DR rate on the same aspects. Notably, in the absence of DG integration, DR has a negligible effect on the voltage profile and CO2 emission in comparison with the base case.

4.4 Case 4

In this scenario, the analysis focuses on incorporating DGs into DR coordination and planning, considering various system constraints. The integration of DGs with DR scheduling significantly enhances the benefits provided by DGs. Additionally, system performance improves with higher DR rates, even in the presence of smaller DGs. Notably, the yearly energy loss shows a substantial decrease, ranging from 29.03 to 33.31%, depending on the DR rates, and the lowest mean voltage experiences a significant increase compared to cases 1 and 2.

Furthermore, when comparing the results of using DGs alone, the difference between maximum-to-minimum demand decreases considerably, leading to a more balanced load profile. Figures 12, 13, and 14 demonstrate the impact of DGs and a 10% DR rate on demand, voltage, and active power losses, respectively. Similarly, Figs. 15, 16, and 17 illustrate the impact of DGs and a 20% DR rate on demand, voltage, and active power losses, respectively. The CO_2 emission for DR rate 10 and 20% are 29.31 and 24.87% respectively.

4.5 Case 5

A study was conducted to evaluate the impact of BESS on the optimal allocation of DGs. The findings, presented in Table 3, show the determined placement and dimensions of the BESS. The planning and scheduling of BESS charging and discharging were strategically executed to improve the voltage profile and reduce energy losses in the network. Coordinating the ideal BESS with DGs aimed to minimize the adverse effects of excessive penetration. The results in Table 2 demonstrate a significant reduction in yearly energy loss (down to 42%) and a flatter load curve compared to a previous case (case-2).

Furthermore, the application of BESS resulted in a remarkable increase in the optimum DG penetration (90.93% as opposed to 69.44%). Figures 18, 19, 20 and 21 showcase the impact of DGs and BESS on the demand pattern, voltage profile, active power losses, and BESS energy storage. The CO_2 emission is reduced by 32.47% in comparison with the base case.

4.6 Case 6

In this situation, the coordination between the DR aggregator and the BESS integrator is essential for optimizing the allocation of DGs and BESS. It is observed that the sizing of BESS and DG depends on the DR rate. Furthermore, a higher DR rate leads to smaller BESS and DG sizes, enhancing the efficiency of the system and improving the DN functionality. According to Table 3, the most significant reduction in yearly energy loss (46.77% savings) is achieved when combining DG, BESS, and a DR rate of 20%. This study emphasizes the importance of incorporating an appropriate DR rate alongside DGs and BESS to ensure an efficient operation of the DN. Figures 22, 23, 24, 25, 26, 27, 28 and 29 demonstrate the impact of varying DR rates on the synchronization of optimal DG and BESS allocation, including the effects on demand pattern, voltage profile, active

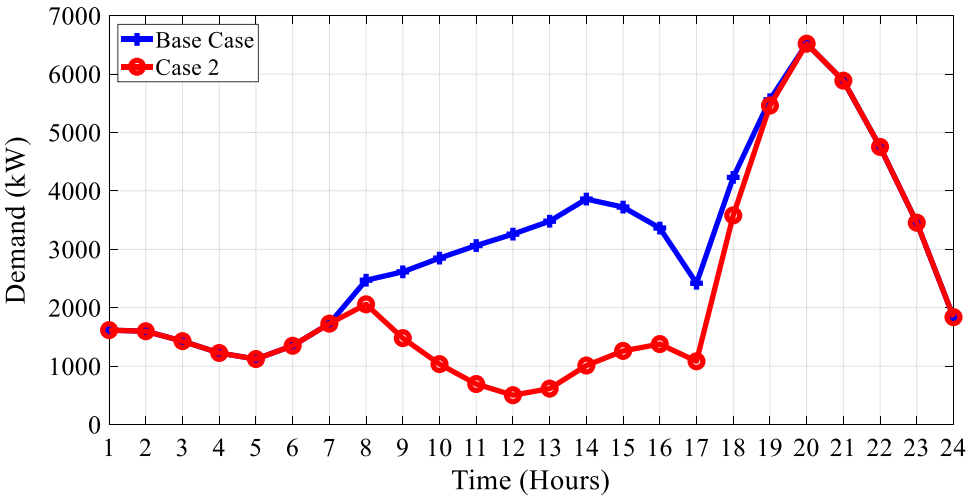

Fig. 5 Impact of DGs on demand pattern

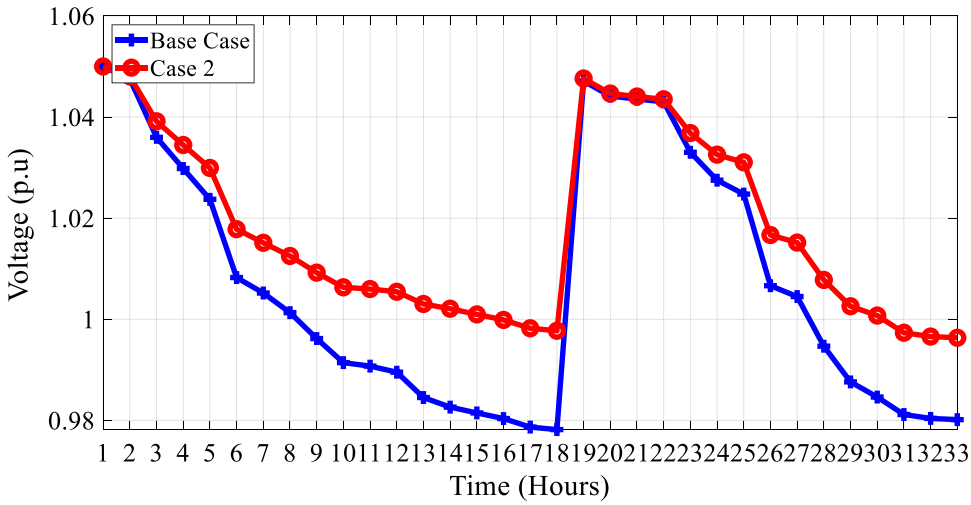

Fig. 6 Impact of DGs on voltage pattern

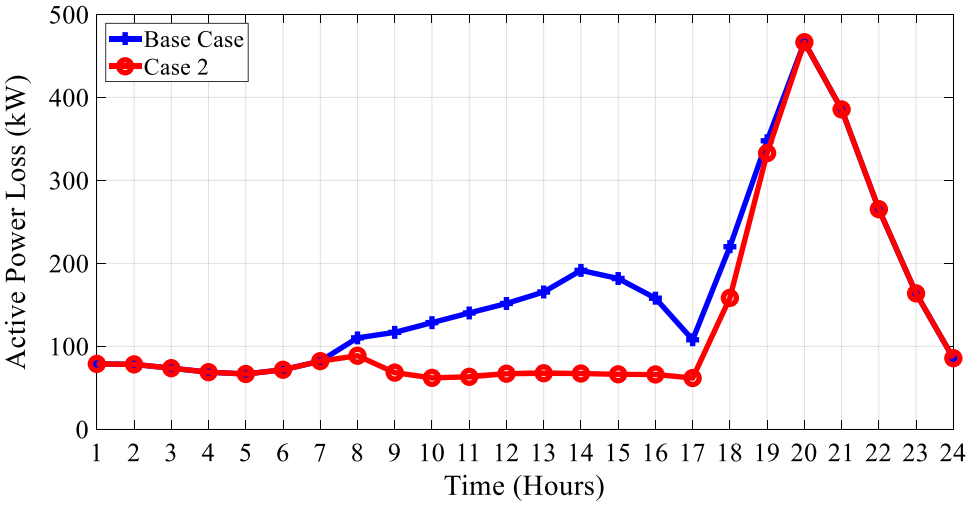

Fig. 7 Impact of DGs on active power losses

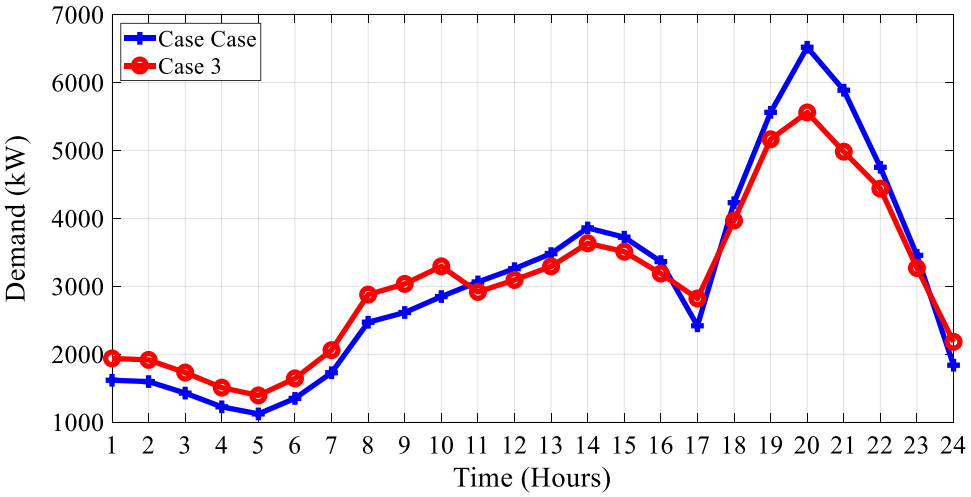

Fig. 8 Impact of 10% DR rate on demand pattern

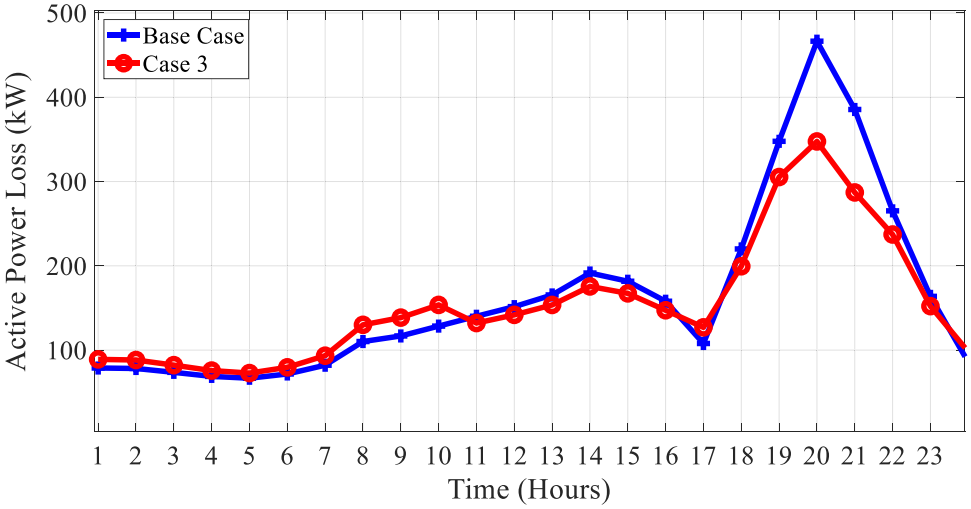

Fig. 9 Impact of 10% DR rate on active power losses

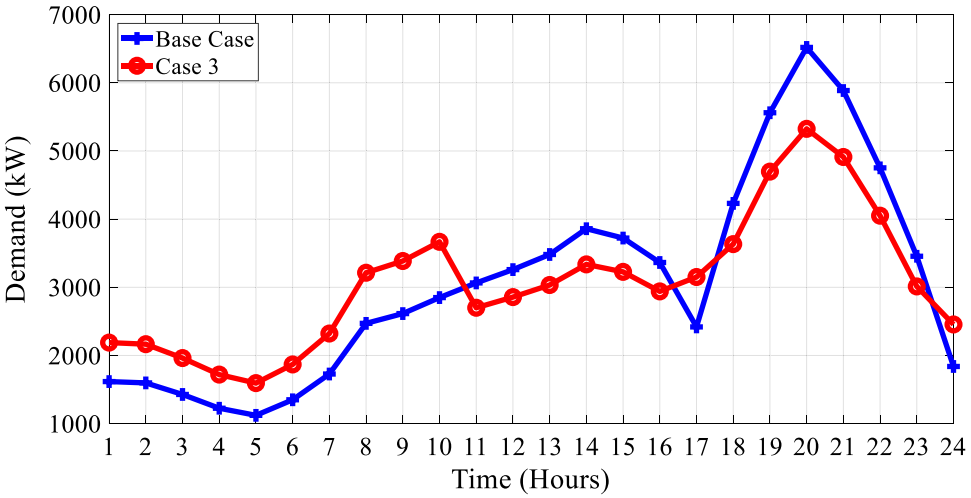

Fig. 10 Impact of 20% DR rate on demand pattern

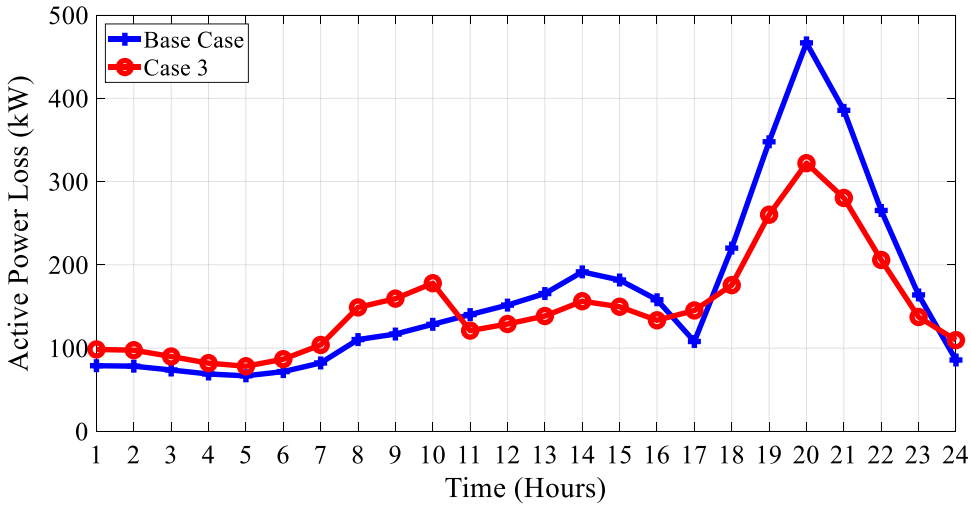

Fig. 11 Impact of 20% DR rate on active power losses

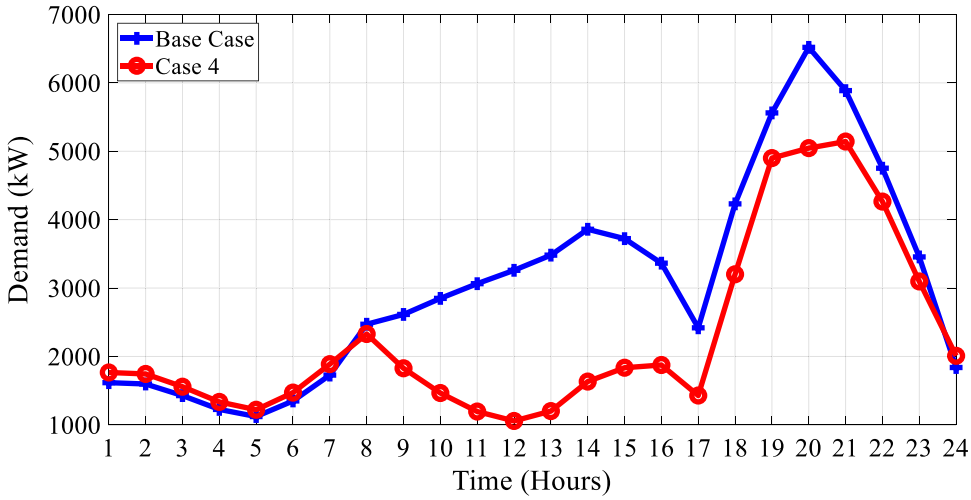

Fig. 12 Impact of DG and 10% DR rate on demand pattern

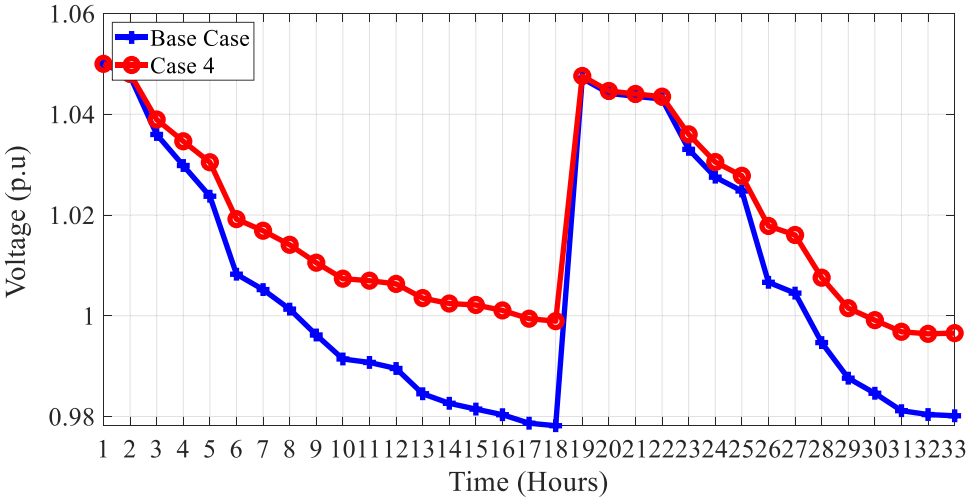

Fig. 13 Impact of DG and 10% DR rate on voltage pattern

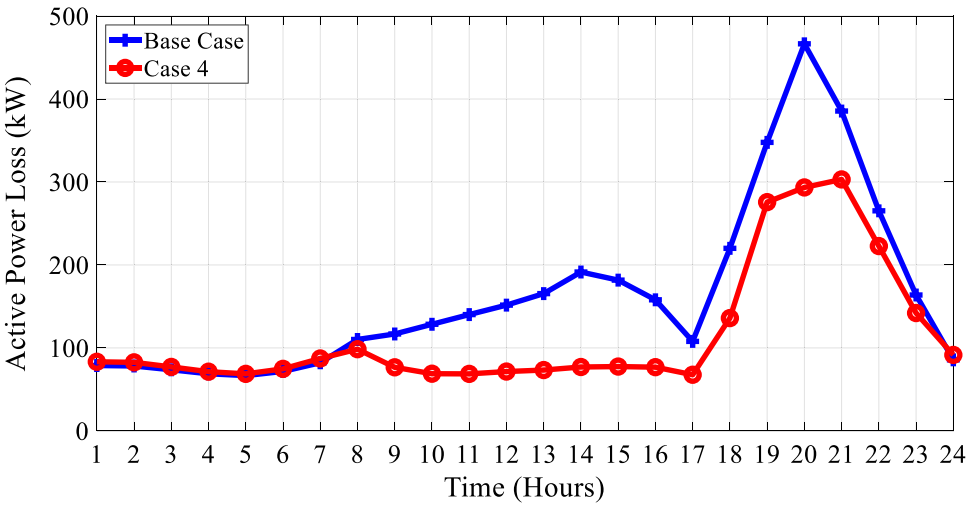

Fig. 14 Impact of DG and 10% DR rate on active power losses

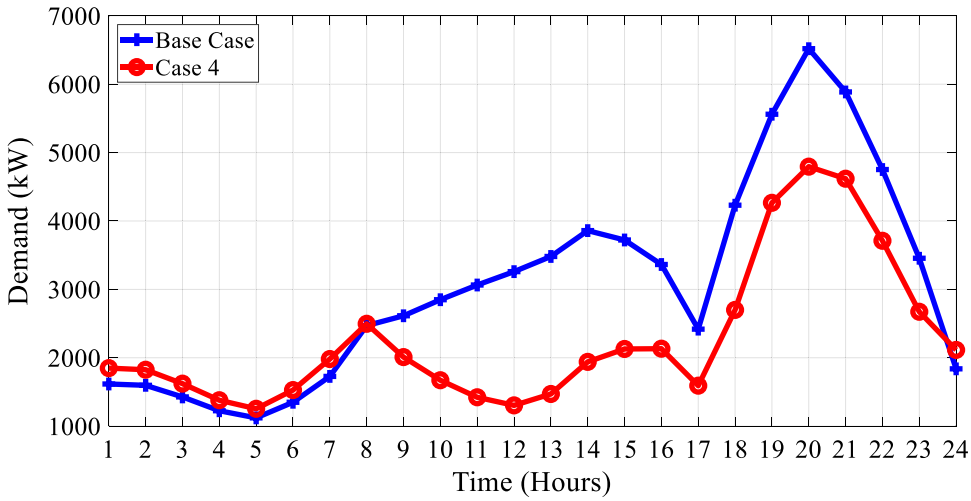

Fig. 15 Impact of DG and 20% DR rate on demand pattern

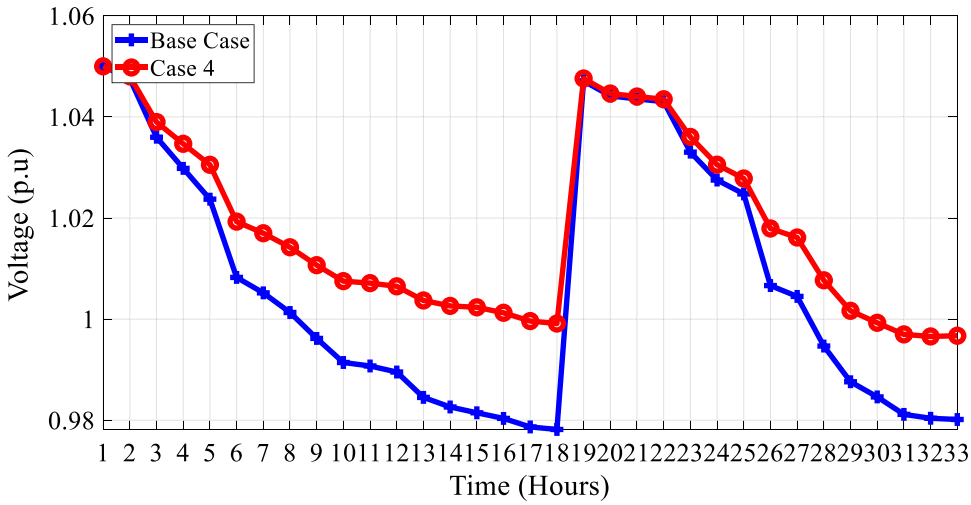

Fig. 16 Impact of DG and 20% DR rate on voltage pattern

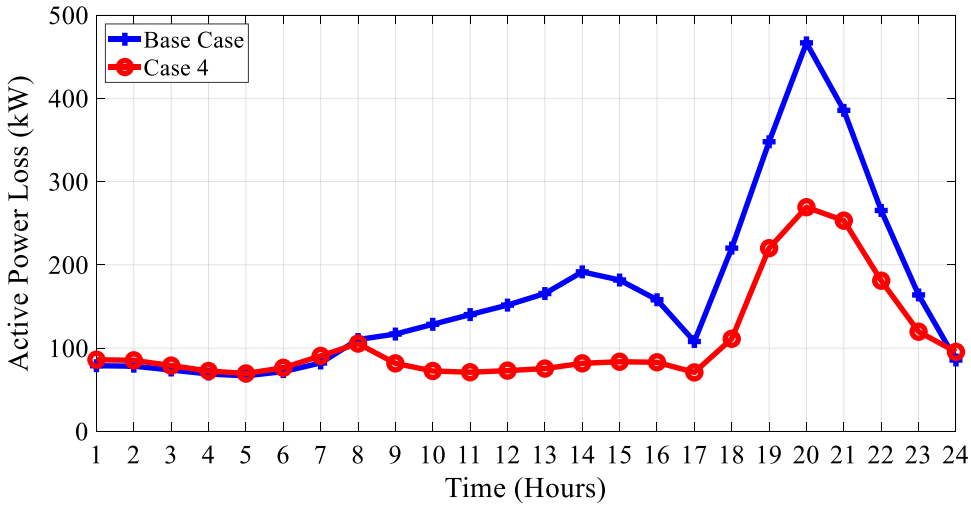

Fig. 17 Impact of DG and 20% DR rate on active power losses

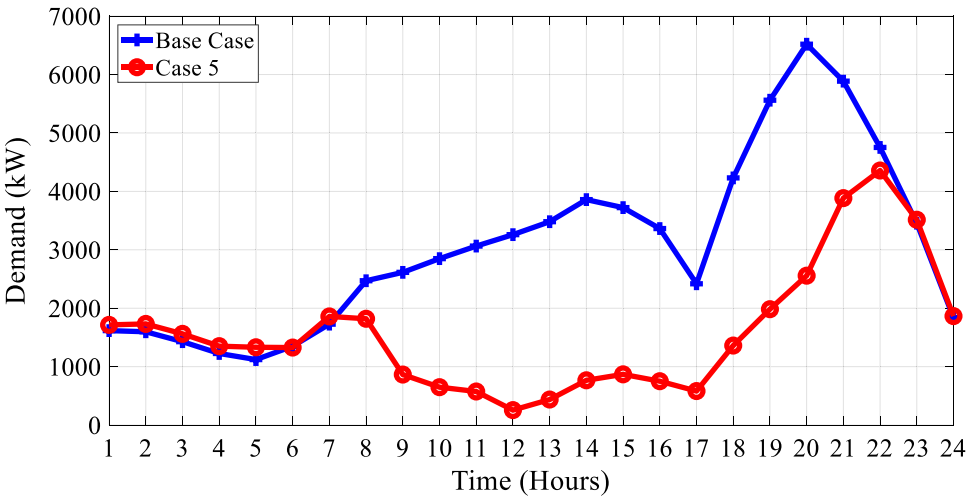

Fig. 18 Impact of DG and BESS on demand pattern

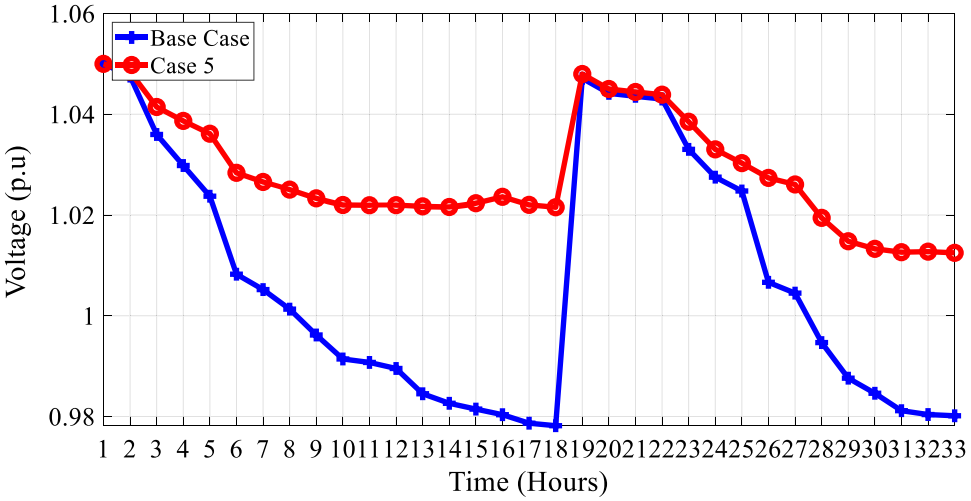

Fig. 19 Impact of DG and BESS on voltage pattern

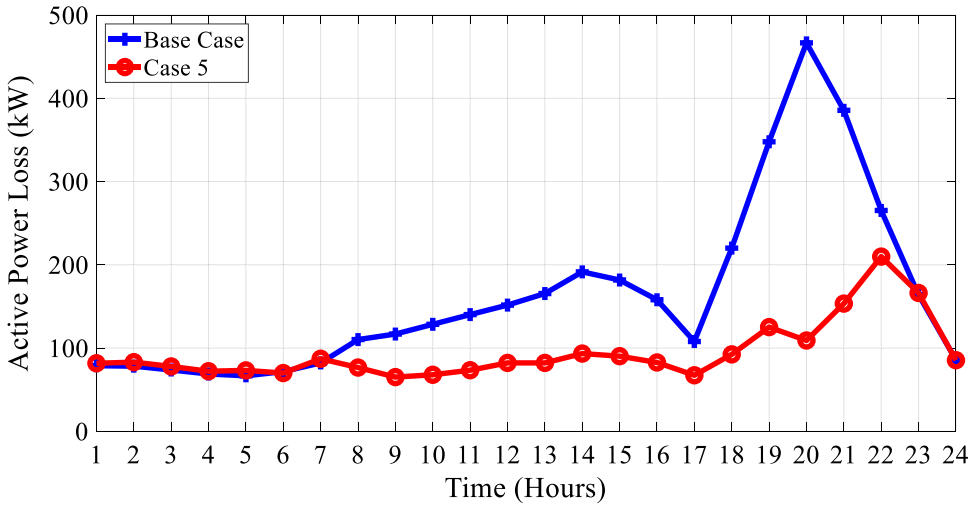

Fig. 20 Impact of DG and BESS on active power losses

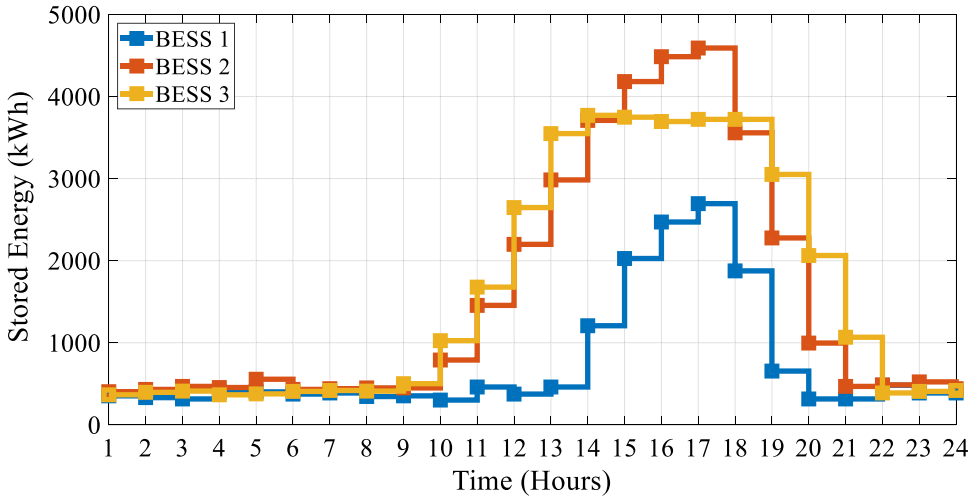

Fig. 21 BESS energy storage (DG + BESS)

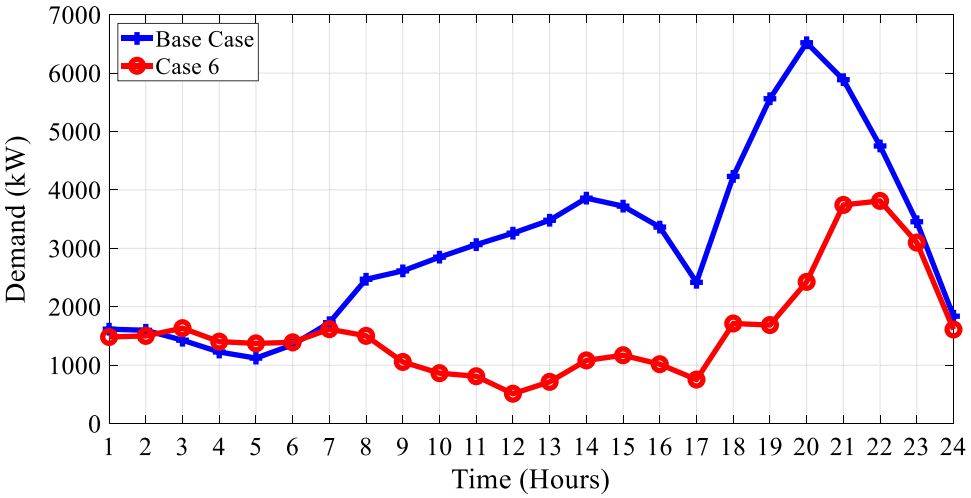

Fig. 22 Impact of DG, BESS and, 10% DR rate on demand pattern

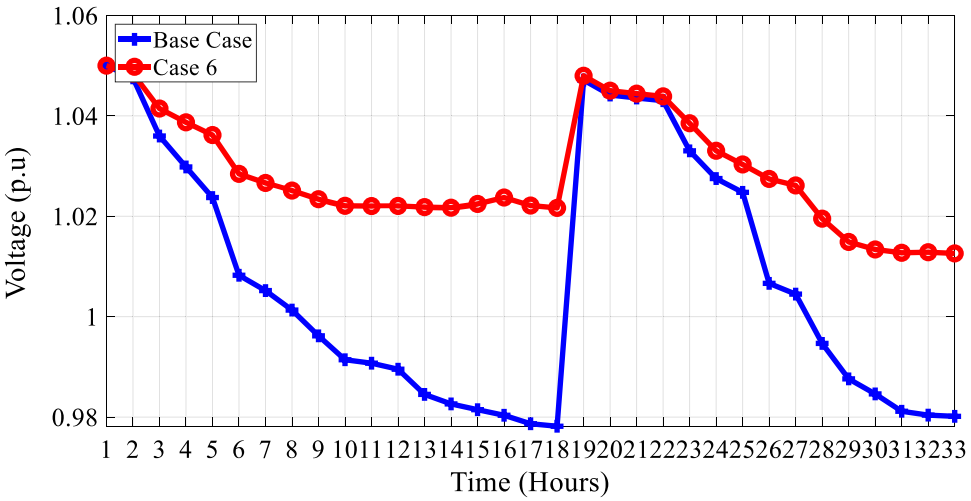

Fig. 23 Impact of DG, BESS and, 10% DR rate on voltage pattern

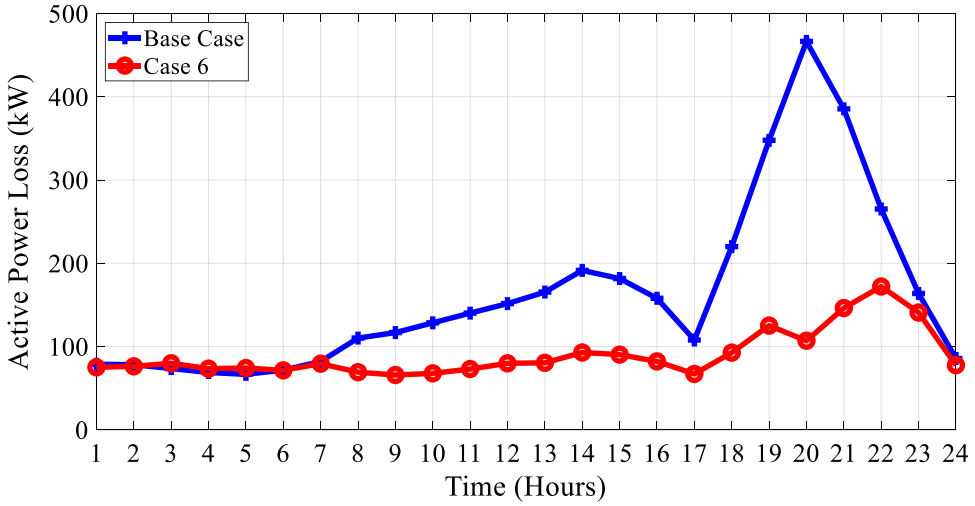

Fig. 24 Impact of DG, BESS and, 10% DR rate on active power losses

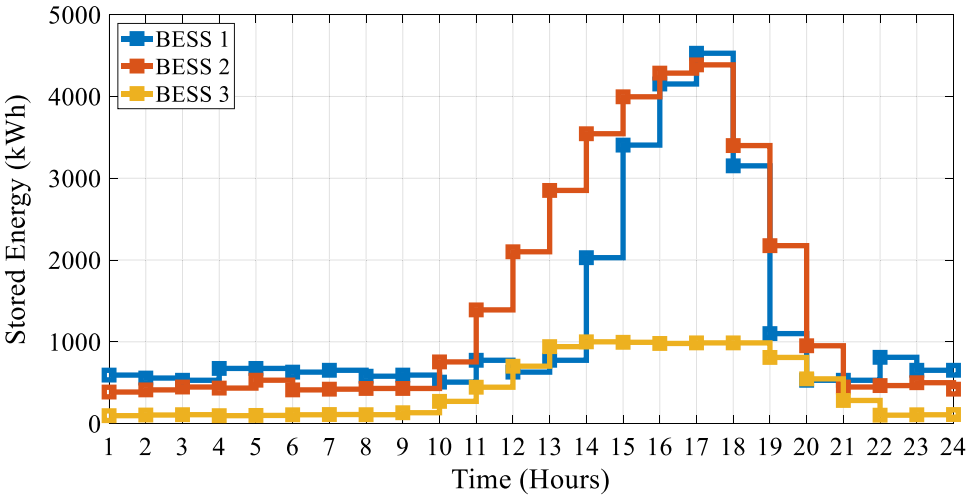

Fig. 25 BESS energy storage (DG, BESS and, 10% DR rate)

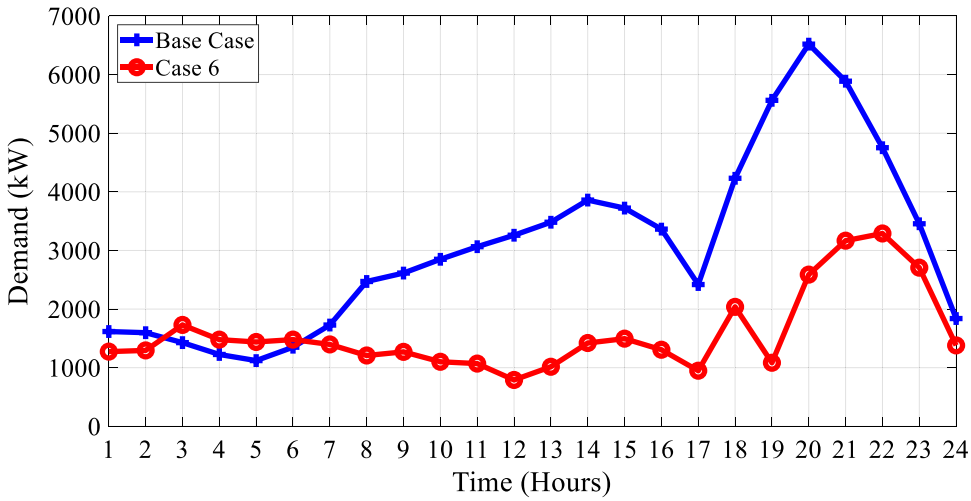

Fig. 26 Impact of DG, BESS, and 20% DR rate on demand pattern

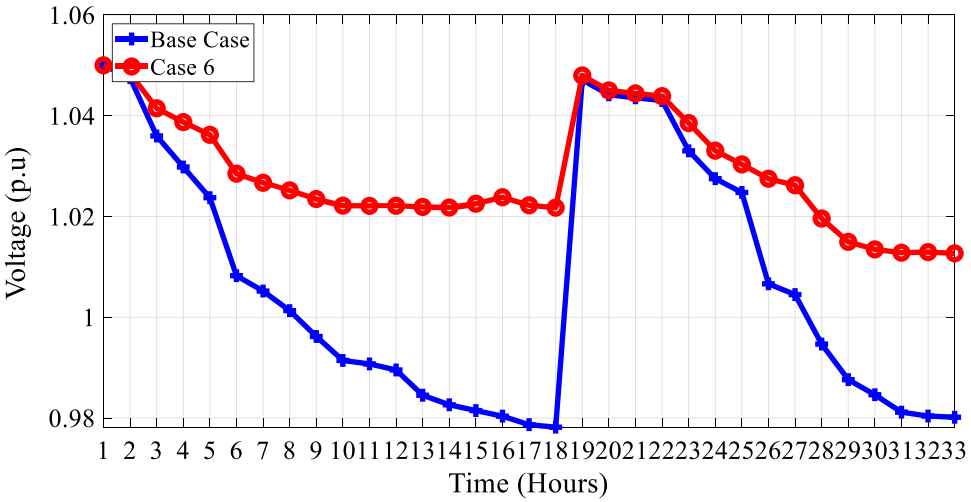

Fig. 27 Impact of DG, BESS, and20% DR rate on voltage pattern

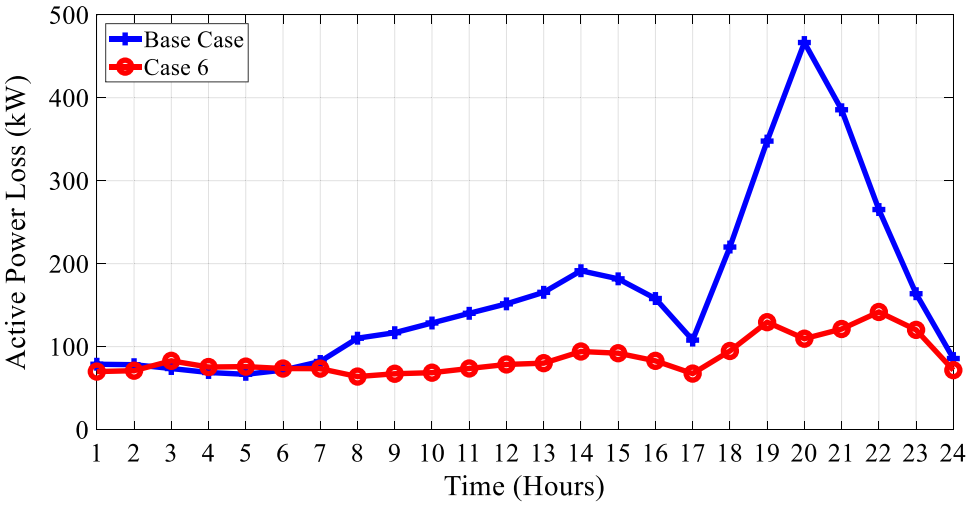

Fig. 28 Impact of DG, BESS and, 20% DR rate on active power losses

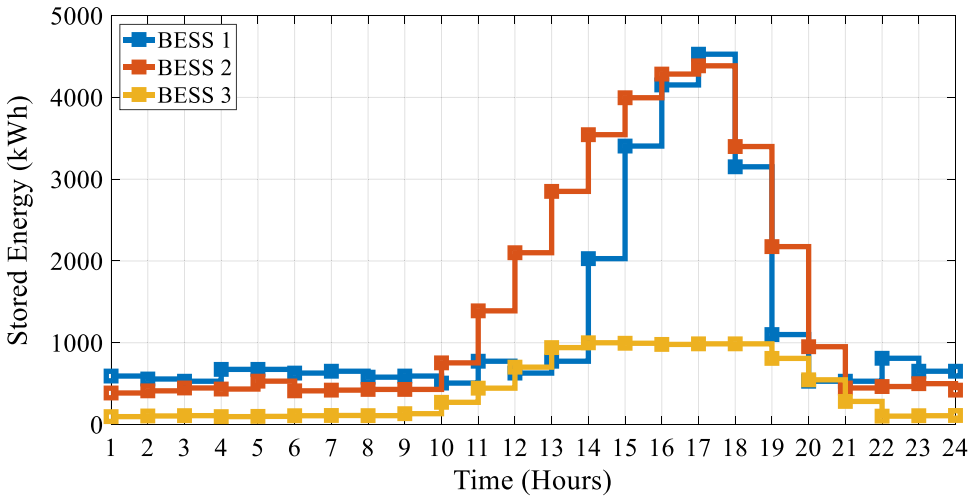

Fig. 29 BESS energy storage (DG, BESS and, 20% DR rate)

power losses, and BESS energy storage. The CO_2 emission is reduced by 32.71% in comparison with the base case.

5 Conclusions

In the context of future DN, three crucial elements are renewable energy utilization, demand DR planning, and the energy storage system. To maximize the technical, financial, and environmental benefits of DN, a well-coordinated optimization approach is proposed in this paper. The methodology focuses on efficiently planning and executing upgrades to the DN. This multilevel optimization system optimizes the coordination of SPV penetration, DR scheduling, and BESS allocation. At level-1, the optimal sizes and locations of DGs and BESS are determined, considering various constraints. At level-2, the DR program is implemented, coordinating with the outcomes from level-1 and dispatching BESS to maintain the balance between renewable energy generation and load demand. To demonstrate the effectiveness of the proposed technique, the IEEE 33 test system is employed. The harmonious integration of DGs, BESS, and DR is explored to achieve the highest possible DN performance. Notably, the performance of DN is significantly impacted by the coordination of different DR rates. In summary, this research highlights the importance of a coordinated approach in future DN, emphasizing the benefits of renewable energy, DR, and energy storage integration.

The implementation of the proposed approach demonstrates that the most substantial reduction in CO_2 emissions (32.71%) is achieved through the coordination of DG, BESS, and a 20% DR rate. Simultaneously, the maximum penetration of renewable energy (89.96%) is attained through the optimal allocation of DG in the coordination with BESS (Figs. 30 and 31).

i. In terms of performance, DGs prove to be highly effective in reducing annual energy losses. However, they do not consistently improve the load profile, and in some cases, may even have a negative impact on it. Furthermore, increased DG penetration can lead to voltage level surges and potential reverse power flow to the grid, setting a limit on their integration into the DS.
ii. Besides improving the load profile and voltage profile while minimizing energy losses, the inclusion of BESS enables higher DG penetration.
iii. Implementing DR successfully levels the load profile, reducing the gap between peak and minimum demand. This eases stress on the system and provides additional benefits, such as reduced reliance on BESS. Consequently, lower BESS deployment leads to a lower DG penetration. Conversely, if PV and BESS penetration is expected to be lower, a higher DR rate offers an efficient means to enhance DS efficiency.
iv. It can be deduced that a higher DR rate relative to optimal results leads to lower DG penetration. A decreased DG power dispatch results in lower energy loss minimization, and a high DR value may negatively impact the system. Hence, a coordinated approach among DGs, BESS, and DR within the DS is crucial.
v. While integrating a Solar PV system into the network can lead to a reduction in CO_2 emissions, the most favorable outcomes in terms of both CO_2 emissions and power quality parameters are achieved when implementing the proposed framework.
vi. The DR scheme exhibits a minimal impact on CO_2 emission reduction when implemented independently. However, its effectiveness significantly improves when integrated into a coordinated system with renewable DG and BESS.

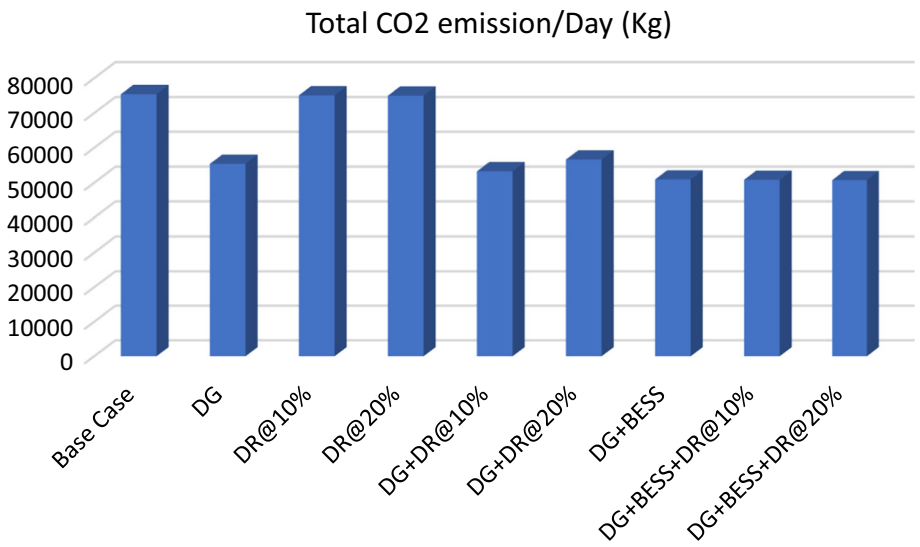

Fig. 30 Total CO_2 emission/day

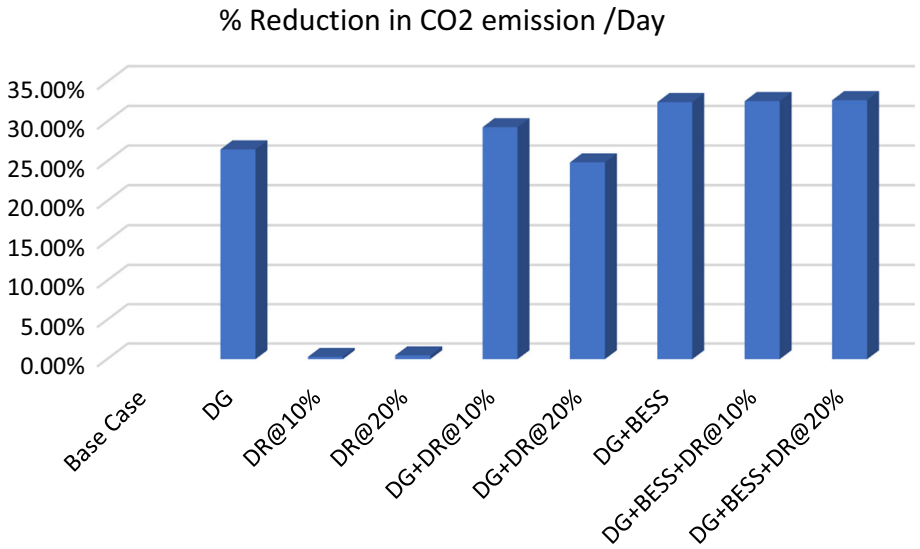

Fig. 31 Reduction in CO_2 emission by CPP

Author contributions Credit Author Statement Vivek Saxena: Conceptualization, Methodology, Software, Data curation, Writing- Original draft preparation, Visualization, Investigation, Validation, Writing-Reviewing and Editing. Narendra Kumar: Supervision Uma Nangia: Supervision

Funding This research received no external funding.

Declarations

Conflict of interest The authors declare no conflict of interest.

References

1. Saxena V, Kumar N, Nangia U (2007) Smart grid: a sustainable smart approach. In: Journal of physics: conference series, p 012042
2. Parsa Moghaddam M, Abdollahi A, Rashidinejad M (2011) Flexible demand response programs modeling in competitive electricity markets. Appl Energy 88(9):3257–3269
3. Medina J, Muller N, Roytelman I (2010) Demand response and distribution grid operations: opportunities and challenges. IEEE Trans Smart Grid 1(2):193–198
4. Saxena V, Kumar N, Nangia U (2021) Analysis of smart electricity grid framework unified with renewably distributed generation. In: Advances in smart communication and imaging systems. Lecture Notes in Electrical Engineering, pp 735–751
5. Hung DQ, Mithulananthan N (2013) Multiple distributed generator placement in primary distribution networks for loss reduction. IEEE Trans Ind Electr 60(4):1700–1708
6. Esmaili M (2013) Placement of minimum distributed generation units observing power losses and voltage stability with network constraints. IET Gener Transm Distrib 7(8):813–821
7. Georgilakis PS, Hatziargyriou ND (2013) Optimal distributed generation placement in power distribution networks: models, methods, and future research. IEEE Trans Power Syst 28(3):3420–3428

8. Saxena V, Kumar N, Nangia U (2022) Recent trends in the optimization of renewable distributed generation: a review. Ing Investig 42(3):e97702
9. Hashemi S, Stergaard J, Yang G (2014) A scenario-based approach for energy storage capacity determination in LV grids with high PV penetration. IEEE Trans Smart Grid 5(3):1514–1522
10. Zheng Y, Dong ZY, Luo FJ, Meng K, Qiu J, Wong KP (2014) Optimal allocation of energy storage system for risk mitigation of discos with high renewable penetrations. IEEE Trans Power Syst 29(1):212–220
11. Zheng Y, Hill DJ, Dong ZY (2017) Multi-agent optimal allocation of energy storage systems in distribution systems. IEEE Trans Sustain Energy 8(4):1715–1725
12. Barcellona S, Piegari L, Musolino V, Ballif C (2018) Economic viability for residential battery storage systems in grid-connected PV plants. IET Renew Power Gener 12(2):135–142
13. Paliwal NK, Singh AK, Singh NK, Kumar P (2018) Optimal sizing and operation of battery storage for economic operation of hybrid power system using artificial bee colony algorithm. Int Trans Electr Energy Syst 29(1):e2685
14. Nick M, Cherkaoui R, Paolone M (2018) Optimal planning of distributed energy storage systems in active distribution networks embedding grid reconfiguration. IEEE Trans Power Syst 33(2):1577–1590
15. Banguero E, Correcher A, Navarro P, Morant F, Aristizabal A (2018) A review on battery charging and discharging control strategies. Appl Renew Energy Syst Energies 11(4):1021
16. Safdarian A, Fotuhi-Firuzabad M, Lehtonen M (2016) Benefits of demand response on operation of distribution networks: a case study. IEEE Syst J 10(1):189–197
17. Cresta M, Gatta FM, Geri A, Maccioni M, Mantineo A, Paulucci M (2015) Optimal operation of a low-voltage distribution network with renewable distributed generation by NaS battery and demand response strategy: a case study in a trial site. IET Renew Power Gener 9(6):549–556
18. Roscoe AJ, Ault G (2010) Supporting high penetrations of renewable generation via implementation of real-time electricity pricing and demand response. IET Renew Power Gener 4(4):369–382
19. Sharma S, Niazi KR, Verma K, Rawat T (2020) Coordination of different DGs, BESS and demand response for multi-objective optimization of distribution network with special reference to Indian power sector. Int J Electr Power Energy Syst 121:106074
20. Sharma S, Niazi KR, Verma K, Rawat T (2020) A bi-level optimization framework for investment planning of distributed generation resources in coordination with demand response. Energy Sources Part A Recovery Util Environ Effects. https://doi.org/10.1080/15567036.2020.1758248
21. Sharma S, Niazi KR, Verma K, Rawat T (2020) Impact of battery energy storage, controllable load and network reconfiguration on contemporary distribution network under uncertain environment. IET Gener Transm Distrib 14(21):4719–4727
22. Yang C, Wu Z, Li X, Fars A (2024) Risk-constrained stochastic scheduling for energy hub: integrating renewables, demand response, and electric vehicles. Energy 288:129680
23. Shen Y, Xie J, He T, Yao L, Xiao Y (2023) CEEMD-fuzzy control energy management of hybrid energy storage systems in electric vehicles. IEEE Trans Energy Convers. https://doi.org/10.1109/TEC.2023.3306804
24. Li R, Xu D, Tian H, Zhu Y (2023) Multi-objective study and optimization of a solar-boosted geothermal flash cycle integrated into an innovative combined power and desalinated water production process: application of a case study. Energy 282:128706
25. Cao B, Dong W, Lv Z, Gu Y, Singh S, Kumar P (2020) Hybrid microgrid many-objective sizing optimization with fuzzy decision. IEEE Trans Fuzzy Syst 28(11):2702–2710
26. Tian H, Li R, Salah B, Thinh P-H (2023) Bi-objective optimization and environmental assessment of SOFC-based cogeneration system: performance evaluation with various organic fluids. Process Saf Environ Prot 178:311–330
27. Li P, Hu J, Qiu L, Zhao Y, Ghosh BK (2022) A distributed economic dispatch strategy for power-water networks. IEEE Trans Control Netw Syst 9(1):356–366
28. Xiao T, Lin Z, Liu C, Liu L, Li Q (2023) Integration of desalination and energy conversion in a thermo-osmotic system using low-grade heat: performance analysis and techno-economic evaluation. Appl Therm Eng 223:120039
29. Duan Y, Zhao Y, Hu J (2023) An initialization-free distributed algorithm for dynamic economic dispatch problems in microgrid: modeling, optimization and analysis. Sustain Energy Grids Netw 34:101004
30. Chen H, Wu H, Kan T, Zhang J, Li H (2023) Low-carbon economic dispatch of integrated energy system containing electric hydrogen production based on VMD-GRU short-term wind power prediction. Int J Electr Power Energy Syst 154:109420
31. Shirkhani M, Tavoosi J, Danyali S, Khosravi Sarvenoee A (2023) A review on microgrid decentralized energy/voltage control structures and methods. Energy Rep 10:368–380
32. Li H-M, Li G-X, Li L, Wu J-Z, Yao Z-P, Zhang T (2023) Combustion characteristics and concentration measurement of ADN-based liquid propellant with electrical ignition method in a combustion chamber. Fuel 344:128142
33. Liu K, Sheng W, Li Z, Liu F, Liu Q, Huang Y, Li Y (2023) An energy optimal schedule method for distribution network considering the access of distributed generation and energy storage. IET Gener Transm Distrib 17:2996–3015
34. Nosratabadi SM, Hooshmand RA, Gholipour E, Parastegari M (2016) A new simultaneous placement of distributed generation and demand response resources to determine virtual power plant. Int Trans Electr Energy Syst 26(5):1103–1120
35. Eid C, Koliou E, Valles M, Reneses J, Hakvoort R (2016) Time-based pricing and electricity demand response: existing barriers and next steps. Util Policy 40:15–25
36. Zhang C, Xu Y, Dong ZY, Wong KP (2017) Robust coordination of distributed generation and price-based demand response in microgrids. IEEE Trans Smart Grid 9(5):4236–4247
37. CEA Report (2023) https://cea.nic.in/wpcontent/uploads/baseline/2023/01/Approved_report_emission__2021_22.pdf
38. Rajput SK, Dheer DK (2022) Integration of 100-kWp PV with low-voltage distribution power system in composite climate: performance and energy metrics analysis. Int J Ambient Energy 43:8176–8192
39. Meena NK, Parashar S, Swarnkar A, Gupta N, Niazi KR (2018) Improved elephant herding optimization for multiobjective DER accommodation in distribution systems. IEEE Trans Ind Inf 14(3):1029–1039

40. Kanwar N, Gupta N, Niazi KR, Swarnkar A (2015) Improved meta-heuristic techniques for simultaneous capacitor and DG allocation in radial distribution networks. Int J Electr Power Energy Syst 73:653–664
41. Saxena V, Kumar N, Nangia U (2022) An impact assessment of distributed generation in distribution network. In: Artificial intelligence and sustainable computing, pp 33–46
42. Safdarian A, Degefa MZ, Lehtonen M, Fotuhi-Firuzabad M (2014) Distribution network reliability improvements in presence of demand response. IET Gener Transm Distrib 8(12):2027–2203
43. Saxena V, Kumar N, Nangia U (2022) An extensive data-based assessment of optimization techniques for distributed generation allocation: conventional to modern. Arch Comput Methods Eng 1–27
44. Baran ME, Wu FF (1989) Network reconfiguration in distribution systems for loss reduction and load balancing. IEEE Trans Power Deliv 4(2):1401–1407
45. Mazidi M, Zakariazadeh A, Jadid S, Siano P (2014) Integrated scheduling of renewable generation and demand response programs in a microgrid. Energy Conver Manag 86:1118–1127